Am J Transl Res 2025;17(7):5332-5343
www.ajtr.org /ISSN:1943-8141/AJTR0166053

*Original Article*

# Endothelial progenitor cell-derived microvesicles therapy relieves myocardial infarction symptoms by altering left ventricular protein expression

Yanling Song[1*], Shuai Wang[2*], Huade Mai[3], Minghui Chen[1], Yunyun Lin[1], Huajun Wu[1], Shenhong Gu[1]

*[1]Department of General Practice, The First Affiliated Hospital of Hainan Medical University, 31 Longhua Road, Longhua District, Haikou 570100, Hainan, China; [2]Department of Geriatrics, The First School of Clinical Medicine, Hainan Medical University, 31 Longhua Road, Longhua District, Haikou 570100, Hainan, China; [3]Department of Geriatrics, The First Affiliated Hospital of Hainan Medical University, 31 Longhua Road, Longhua District, Haikou 570100, Hainan, China. [*]Equal contributors.*

Received May 15, 2025; Accepted July 8, 2025; Epub July 15, 2025; Published July 30, 2025

**Abstract:** Objective: To investigate the therapeutic potential of endothelial progenitor cell-derived microvesicles (EPC-MVs) in a rat myocardial infarction (MI) model, focusing on their effects on inflammation, apoptosis, and global proteomic changes in the left ventricle. Methods: Endothelial progenitor cells (EPCs) were isolated from mouse bone marrow, and microvesicles (MVs) were derived and injected into rats with MI induced by ligation of the left anterior descending artery. Therapeutic efficacy was assessed by measuring inflammatory cytokines (TNF-α, IL-6) and cardiac injury markers (creatine kinase-MB, myoglobin), along with histologic and apoptotic analyses. A global proteomic analysis of left ventricular tissue was performed to explore the underlying molecular mechanisms. Key targets, including components of the NLRP3 inflammasome (NLRP3, Caspase-1, apoptosis-associated speck-like protein containing a CARD), were validated by western blotting. Results: EPC-MV treatment significantly reduced MI-induced cardiac injury, as evidenced by decreased inflammatory cytokines and cardiac injury markers, preservation of myocardial architecture, reduced fibrosis, and suppression of cardiomyocyte apoptosis. Proteomic analysis revealed significant alterations in inflammatory and metabolic pathways, supported by KEGG and Reactome enrichment analyses. Molecular validation confirmed that EPC-MVs inhibited the activation of the NLRP3 inflammasome and downregulated downstream effectors, including IL-6 and atrial natriuretic peptide. Conclusion: EPC-MVs alleviated myocardial ischemic injury by remodeling the cardiac proteome, suppressing inflammatory and apoptotic signaling. These results position EPC-MVs as a promising cell-free therapeutic strategy for MI.

**Keywords:** Myocardial infarction, endothelial progenitor cell-derived microvesicles, proteomics, apoptosis, cardiac repair, left ventricle remodeling

## Introduction

Myocardial infarction (MI) is caused by ischemic necrosis of the myocardium, typically resulting from the sudden blockage of a coronary artery [1]. Left ventricular infarction is the most common form of MI. Clinical manifestations include severe, prolonged chest pain, fever, frequent nausea and vomiting, and, in severe cases, arrhythmias, shock, and heart failure, all of which present significant life-threatening risks [2]. Post-MI cardiac repair occurs in two phases: the early inflammatory phase, which lasts up to 72 hours, and the subsequent proliferative phase, which occurs beyond this period [3, 4]. The early phase is characterized by infarct expansion due to collagen degradation between cardiomyocytes, facilitated by serine proteases and matrix metalloproteinases (MMPs) [4]. In the later stages, ventricular remodeling involves both cellular and molecular changes, including oxidative stress, apoptosis, myocardial hypertrophy, neurohormonal responses, ventricular dilation, and scar tissue formation [5].

Endothelial progenitor cells (EPCs), precursors of vascular endothelial cells, are capable of

https://doi.org/10.62347/ZJ0X1177

migrating to ischemic regions and promoting angiogenesis through differentiation and proliferation, thereby enhancing blood flow to ischemic tissues [6]. Additionally, EPCs suppress T cell proliferation and shift their phenotype to a more regulatory, less pro-inflammatory profile, contributing to the formation of immunosuppressive blood vessels [7].

Previous studies have emphasized the therapeutic potential of EPC transplantation, particularly when delivered to the marginal zone of MI, significantly enhancing regenerative outcomes [8]. The quantity and functional integrity of EPCs are closely associated with endothelial cell (EC) injury and dysfunction, making EPCs crucial clinical biomarkers for assessing vascular health and cumulative cardiovascular risk [9]. EPCs facilitate post-MI cardiac repair through immunomodulation, neovascularization, extracellular matrix remodeling, and microenvironmental adaptation. EPC characterization typically involves surface markers such as CD133, CD34, and VEGFR-2 (also known as KDR or Flk-1).

Microvesicles (MVs), small extracellular membrane fragments released by apoptotic or activated cells, are produced by various sources including platelets, ECs, and EPCs. These MVs play a critical role in cellular activation, stress responses, and apoptosis regulation [10]. MVs, with distinct surface markers indicating their cellular origin, have beneficial properties, including anti-inflammatory, anticoagulant, and pro-angiogenic functions. Notably, EPC-derived MVs have been shown to protect cardiomyocytes from angiotensin II-induced hypertrophy and apoptosis, enhance endothelial performance, modulate angiogenic pathways, and reduce oxidative stress-induced endothelial dysfunction [11, 12].

Following vascular or tissue injury, circulating EPCs are mobilized to the damaged site, contributing to vascular regeneration through angiogenesis (the extension of pre-existing endothelial cells) and vasculogenesis (the *de novo* formation of blood vessels) [13, 14]. Simultaneously, EPC-derived soluble factors, along with exosomes and MVs, play a crucial role in mitigating adverse microenvironmental conditions, such as oxidative stress and inflammation [15]. These bioactive molecules regulate cellular survival and apoptosis, inhibit mesenchymal cell transformation and fibrosis [16], guide the migration of stem and progenitor cells [17], support cardiomyocyte (CM) viability, and promote angiogenesis [18]. Together, these mechanisms facilitate tissue repair and regeneration. This study investigates the therapeutic potential of EPC-derived MVs in modulating inflammation and promoting cardiomyocyte repair, focusing on the associated signaling pathways.

## Materials and methods

### *Experimental animals*

All experiments were conducted using a cohort of thirty C57BL/6 mice (8-12 weeks old, 20-25 g body weight), obtained from Charles River Laboratories. The mice were housed in a controlled environment with *ad libitum* access to standard rodent chow and water. Mice were randomized into their respective experimental groups, and data collection and analysis were performed by investigators blinded to treatment assignments. All animal procedures were carried out in strict accordance with the Guide for the Care and Use of Laboratory Animals by the National Institutes of Health. The study protocol was approved by the Institutional Animal Care and Use Committee (IACUC) at Hainan Medical College (Approval No. HYLL-2022-148), and all invasive procedures were performed under anesthesia to minimize animal suffering.

### *Extraction, isolation and identification of EPCs*

Bone marrow was collected by flushing the tibias and fibulas of euthanized mice with phosphate-buffered saline (PBS) after sterile removal of surrounding muscle and connective tissue. The resulting single-cell suspension was seeded onto culture plates pre-coated with human fibronectin and cultured in EGM-2MV medium at 37°C. The culture medium was replaced every 48 hours, and after approximately one week, adherent endothelial progenitor cells (EPCs) were harvested for subsequent analysis.

EPC phenotype was characterized using multicolor flow cytometry. Cells were incubated for 30 minutes at 4°C with a panel of fluorophore-conjugated primary antibodies: CD34-FITC, von Willebrand factor-FITC, VEGFR-2-PE, CD133-

APC, and CD45-PC7. All antibodies were used according to the concentrations recommended by the respective manufacturers (Beckman Coulter, R&D Systems, Miltenyi, BD Pharmingen). Specificity was confirmed using fluorophore-matched mouse IgG antibodies as isotype controls. After staining, cells were washed with Hanks' balanced salt solution (HBSS), pelleted by centrifugation (1400 rpm, 10 min), and analyzed on a FACSAria™ flow cytometer (BD Biosciences) to quantify marker expression as a percentage of the total cell population.

This protocol consistently yielded approximately $1 \times 10^8$ mononuclear cells per mouse. The EPC population, defined as $CD34^+/CD133^+/VEGFR\text{-}2^+$, represented about 0.03% of the total cell count, resulting in an EPC-to-mononuclear cell ratio of approximately 1:3,000, providing an adequate source for subsequent microvesicle isolation.

To isolate MVs, EPCs were cultured to 80% confluency and conditioned in serum-free medium for 24 hours. The collected supernatant underwent a differential centrifugation protocol at 4°C, starting with 300×g for 5 minutes and 2,000×g for 15 minutes to remove cells and debris. The cleared supernatant was then ultracentrifuged at 100,000×g for 2 hours. The resulting EPC-MV pellet was washed in PBS and centrifuged again at 100,000×g for 1 hour. The morphology of isolated EPC-MVs was observed using an FEI Tecnai-10 transmission electron microscope after fixation, dehydration, and gold sputter-coating. The proteomic identity of the MVs was confirmed by western blotting, verifying the presence of the EPC surface marker CD34, ensuring preparation quality for therapeutic applications.

*Preparation of the animal model*

The experimental design included four groups: Control group: No intervention, n = 5; Sham group: Chest puncture without left anterior descending (LAD) ligation, followed by 50 μg PBS administration on postoperative days 3 and 7, n = 5; MI group: Thoracotomy, LAD puncture, and ligation under 4% isoflurane anesthesia, followed by 50 μg PBS administration on days 3 and 7 post-surgery, n = 10; EPC-MVs group: MI model with additional treatment of 50 μg EPC-MVs on days 3 and 7, n = 10.

After the study, mice were euthanized with chloral hydrate, and cardiac tissues were collected and stored at -80°C for subsequent analysis.

All animal experiments were conducted following the National Institutes of Health guidelines for laboratory animal welfare and were approved by the Ethics Committee of Hainan Medical College (Approval No. HYLL-2022-148).

*Histologic staining*

Following euthanasia, the hearts of all mice were carefully excised, with three samples from each experimental group selected for histological evaluation. The hearts were bisected transversely between the atrioventricular groove and the apex to ensure consistent sample preparation. The collected tissues were fixed in 4% paraformaldehyde, embedded in paraffin, and sectioned into 4-μm thick cross-sections. Morphologic assessments were conducted using hematoxylin and eosin (H&E) staining, following standardized protocols. Additionally, collagen deposition was assessed by Masson's trichrome staining (Sigma, USA), with collagen fibers visualized in blue, adhering to established guidelines.

Cardiomyocyte death in each experimental group was assessed *in vitro* using a TUNEL immunofluorescence detection kit (Beyotime Biotechnology, China). Apoptotic cardiomyocytes were identified by fluorescence intensity, captured and analyzed using a fluorescence microscope.

*LC-MS/MS analysis*

Left ventricular tissue was harvested from model mice, washed thoroughly with chilled PBS to remove residual blood and contaminants, and then lysed in a buffer containing protease inhibitors to release cellular proteins. After centrifugation to remove insoluble materials, 50 μg of protein was isolated via acetone precipitation. Protein reduction was achieved using 20 mM DTT (Thermo Scientific, USA) in a urea-Tris-HCl-EDTA buffer (pH 8.8, TOYOBO, Japan), and the samples were protected from light during alkylation with iodoacetamide. Proteins were digested with trypsin (Thermo Scientific, USA) overnight at 37°C. Formic acid (American Chemical Society, USA) was then

added to adjust the pH to 2.5, halting enzymatic activity and precipitating DOC. Peptides were desalted using a Sep-Pak C18 column and concentrated.

Peptide separation and identification were conducted by liquid chromatography-tandem mass spectrometry (Agilent, USA), with high-performance liquid chromatographygradient elution facilitating peptide isolation prior to mass spectrometric analysis. In the mass spectrometer, peptides underwent electrospray ionization and were identified based on their mass-to-charge ratios (m/z) and fragment ions. Using tandem mass spectrometry, peptides were sequentially isolated, fragmented by collision-induced dissociation, and analyzed to determine their amino acid sequences.

The resulting mass spectrometry data were processed using bioinformatics tools, aligning the spectra with a protein database to identify the protein composition. Quantitative analysis was performed using a label-free approach, comparing peptide intensities directly across samples. Gene Ontology (GO) and KEGG pathway analyses were applied to interpret proteomic changes in the left ventricular tissue following myocardial infarction. Additionally, a protein-protein interaction network was constructed to map signaling pathways and interprotein relationships.

*ELISA*

Levels of TNF-α, IL-6, lactate dehydrogenase (LDH), myoglobin (MYO/MB), and creatine kinase-MB (CK-MB) were quantified using specific ELISA assay kits, following the manufacturer's instructions. MYO/MB was purchased from AFG Scientific (USA), while the other reagents were sourced from Beyotime Biotechnology (China).

*Western blot detection*

Protein lysates were generated by homogenizing tissue samples or cell pellets in RIPA buffer (Thermo Fisher Scientific) supplemented with a cocktail of protease and phosphatase inhibitors (Roche). Lysates were clarified by centrifugation at 12,000×g for 15 minutes at 4°C, and protein concentration in the supernatant was quantified using a BCA Protein Assay (Thermo Fisher Scientific). For immunoblotting, a standardized protein quantity (20-40 μg) per sample was denatured in 5× Laemmli buffer at 95°C for 10 minutes. Samples were resolved on 10% or 12% SDS-polyacrylamide gels and electroblotted onto polyvinylidene difluoride membranes (Millipore). Membranes were blocked for one hour at room temperature in Tris-buffered saline with 0.1% Tween 20 (TBST) containing 5% non-fat milk to prevent nonspecific antibody binding. The membranes were incubated overnight at 4°C with primary antibodies targeting: CD34 (1:1000, Abcam, ab317588), Bcl-2 (1:2000, Abcam, ab182858), Bax (1:1000, Abcam, ab32503), Cleaved Caspase-3 (1:500, Abcam, ab2302), NLRP3 (1:1000, GeneTex, GTX639954), Caspase-1 (1:1000, GeneTex, GTX101322), ASC (1:1500, MCE, HY-P80548), IL-6 (1:1000, Abcam, ab290735), NPM1 (1:1000, Abcam, ab52644), CSRP3 (1:1000, Abcam, ab172952), NPPA (1:1000, Abcam, ab225844), CCL23 (1:1000, Thermo Fisher Scientific, 500-P124-1MG), and β-actin (1:1000, Abcam, ab8226). After washing with TBST, the membranes were incubated with the corresponding HRP-conjugated secondary antibodies for one hour. Immunoreactive bands were detected using an enhanced chemiluminescence (ECL) substrate (Thermo Fisher Scientific), and signals were captured by a chemiluminescence imaging system. Finally, band intensities were quantified via densitometry using ImageJ software, with protein expression normalized to β-actin as an internal control.

*Statistical analysis*

Statistical analyses were performed using GraphPad Prism 8.0 software. A significance level of $P < 0.05$ was used for all comparisons. For comparisons between two groups, Student's t-test was used, while for comparisons across multiple groups, one-way ANOVA with Tukey's post hoc test was applied. Quantitative data are expressed as mean ± standard error of the mean (SEM), with the number of independent replicates (n) specified in the figure legends. For bioinformatic analyses, pathway enrichment was assessed using a two-tailed hypergeometric test with Benjamini-Hochberg correction for multiple testing.

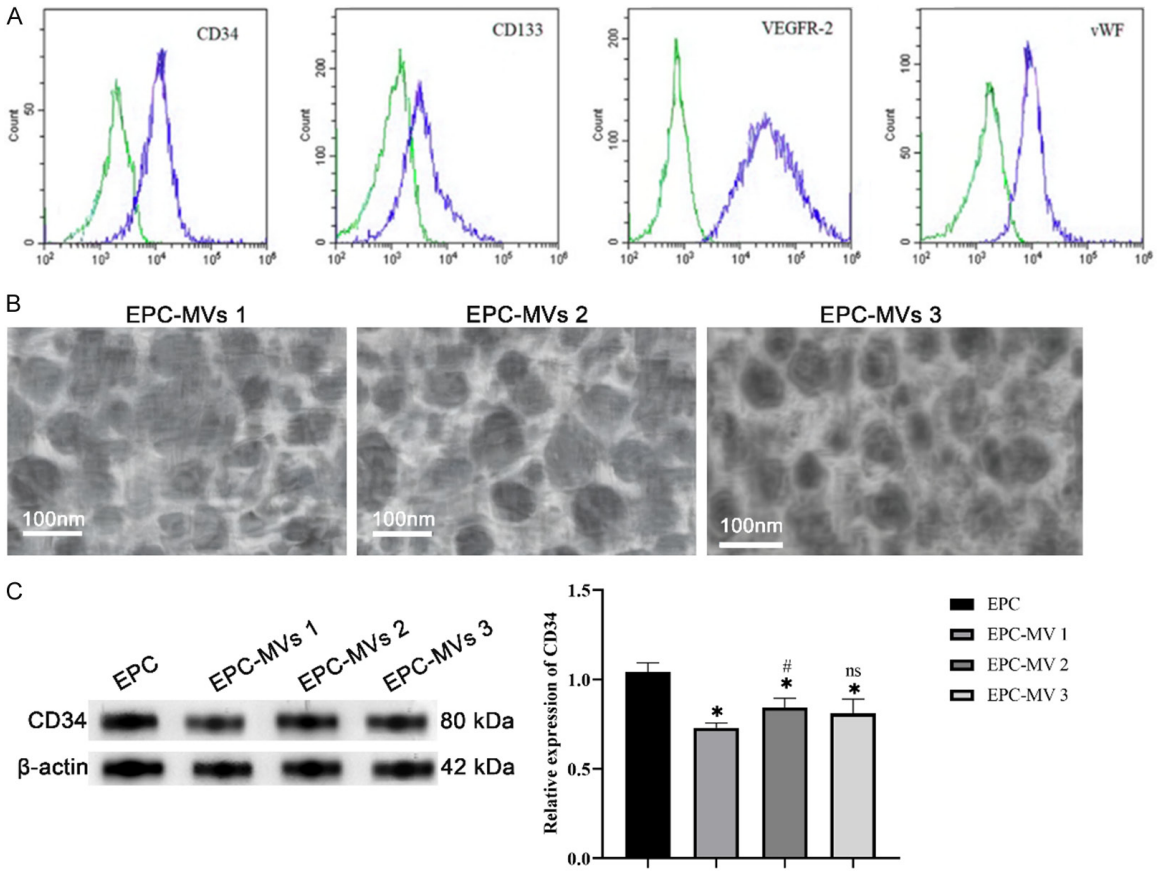


**Figure 1.** Identification of endothelial progenitor cells (EPC) and endothelial progenitor cell-derived microvesicles (EPC-MVs) and the comparison of hematoxylin and eosin (H&E) staining images of heart tissue under different conditions. A. Flow cytometry analysis illustrating the expression of cluster of differentiation 34 (CD34), cluster of differentiation 133 (CD133), vascular endothelial growth factor receptor 2 (VEGFR-2), and von Willebrand factor (vWF) in cultured endothelial progenitor cells (EPCs). Blue curves represent the isotype control, while green curves depict specific markers. Scale bar 100 nm. B. Transmission electron microscopy (TEM) imaging of isolated EPC-derived microvesicles (EPC-MVs), showing spherical structures. The scale bar corresponds to 100 nm. C. Quantification of CD34 protein expression in EPC-derived microvesicles. n = 3 independent biological replicates per group. Student's t-test. *P < 0.05 vs. EPC; ns, not statistically significant, #P < 0.05 vs. EPC-MV 1.

## Results

### *Identification of EPC and EPC-MVs*

In this study, endothelial progenitor cells (EPCs) were successfully isolated and subjected to detailed morphologic and phenotypic characterization at various developmental stages. Flow cytometric analysis confirmed the expression of canonical EPC surface markers - CD133, CD34, and VEGFR-2 - validating the efficacy of the isolation protocol (**Figure 1A**). Transmission electron microscopy revealed distinct ultrastructural differences among microvesicle populations (**Figure 1B**). While the overall morphology was similar, variations in spatial distribution and vesicle density suggested heterogeneity in size and abundance. Western blot analysis confirmed that EPC-MVs retained CD34 expression, distinguishing them from their cellular source and confirming their EPC origin (**Figure 1C**). These vesicles exhibit pro-angiogenic properties, highlighting their therapeutic potential in myocardial infarction and other vascular repair applications.

### *EPC-MVs intervention to alleviate MI tissue damage*

To investigate the cardioprotective mechanisms of EPC-MVs, their therapeutic efficacy was evaluated in a murine MI model. The MI model displayed hallmark features of acute cardiac injury, including a significant increase in

pro-inflammatory cytokines TNF-α (**Figure 2A**) and IL-6 (**Figure 2B**), as well as elevated levels of circulating cardiac damage markers such as CK-MB, MYO/MB (**Figure 2C**), and LDH (**Figure 2D**). Notably, administration of EPC-MVs significantly countered these inflammatory and cytotoxic responses, as evidenced by suppressed cytokine expression and reduced cardiac enzyme levels. Histologic examination further supported the restorative effects of EPC-MVs. In contrast to the extensive myocardial damage observed in untreated MI hearts by H&E staining (**Figure 2F**), Masson's trichrome staining of the EPC-MV-treated hearts revealed significantly reduced interstitial collagen deposition, suggesting a reduction in cardiac fibrosis (**Figure 2G**). While MI induction resulted in an increase in relative heart weight, EPC-MV treatment did not significantly alter this finding (**Figure 2E**). At the cellular level, EPC-MVs exerted potent anti-apoptotic effects, demonstrated by a significant reduction in TUNEL-positive nuclei within the infarct border zone of treated animals (**Figure 2H**). Western blot analysis further substantiated these findings, showing a shift in the balance of apoptotic regulators. Specifically, EPC-MV treatment promoted the expression of the anti-apoptotic protein Bcl-2 while downregulating pro-apoptotic factors BAX and cleaved caspase-3 (**Figure 2I**).

*Proteomic analysis of left ventricle*

To explore the biological significance of the identified proteins, a multi-tiered bioinformatics analysis was conducted. GO enrichment analysis identified Cysteine and Serine-Rich Protein 3 (CSRP3), Nucleophosmin 1 (NPM1), and Atrial Natriuretic Peptide (NPPA) as key mediators of cellular signaling, metabolism, and disease-related functions (**Figure 3A**). These proteins were significantly enriched in pathways relevant to MI pathophysiology, including muscle tissue development and cardiac muscle membrane repolarization (**Figure 3B**). KEGG pathway analysis further highlighted NPPA's involvement in critical MI-associated signaling networks, such as HIF-1, cGMP-PKG, and vascular smooth muscle contraction pathways, which regulate cellular stress and neuroinflammatory responses (**Figure 3C**). The statistical robustness of these findings was supported by high enrichment scores and significant *p*-values (**Figure 3D**). To further explore the functional interactions between these factors, Reactome and WikiPathways analyses were performed. Reactome analysis revealed a complex interaction network involving NPM1, NPPA, and IL16, linking them to essential physiological processes such as cardiac conduction, immune regulation, and cell cycle control (**Figure 4A**, **4B**). Complementary WikiPathways analysis identified specific regulatory roles for NPPA and NPM1 in cardiomyocyte hypertrophy and mRNA processing (**Figure 4C**, **4D**). Together, these bioinformatic analyses converge on a core set of proteins - CSRP3, NPM1, NPPA, and IL16 - as crucial regulators of muscle development, DNA damage response, and vascular integrity in the post-MI environment, linking them to broader regulatory circuits of cardiac function and immune modulation.

*Effect of EPC-MVs on NLRP3 inflammasome-related proteins in MI injury*

To elucidate the molecular mechanisms underlying EPC-MV-mediated cardioprotection, we quantified the expression of key regulatory proteins in cardiac tissue through western blot analysis. MI induced a robust inflammatory response, characterized by significant upregulation of the NLRP3 inflammasome components - NLRP3, Caspase-1, and ASC - along with the cytokine IL-6 (**Figure 5A**). EPC-MV administration effectively suppressed this inflammatory cascade, normalizing the expression of these critical mediators. Moreover, the inflammation-associated protein CCL23, which was elevated after MI, was significantly downregulated by EPC-MV treatment, highlighting their broad immunomodulatory effect (**Figure 5B**).

Beyond their anti-inflammatory action, EPC-MVs also affected proteins involved in myocardial stress and structural integrity. The stress-response protein NPM1, elevated in response to MI, was significantly reduced following EPC-MV treatment. Concurrently, the levels of CSRP3, a protein essential for myocardial architecture and reduced after MI, were restored by EPC-MV administration. This finding underscores the direct role of EPC-MVs in preserving the structural framework of the heart. Interestingly, while MI induced the expression of NPPA, it remained unchanged with EPC-MV treatment, suggesting that NPPA may serve as a general cardiac stress marker rather than

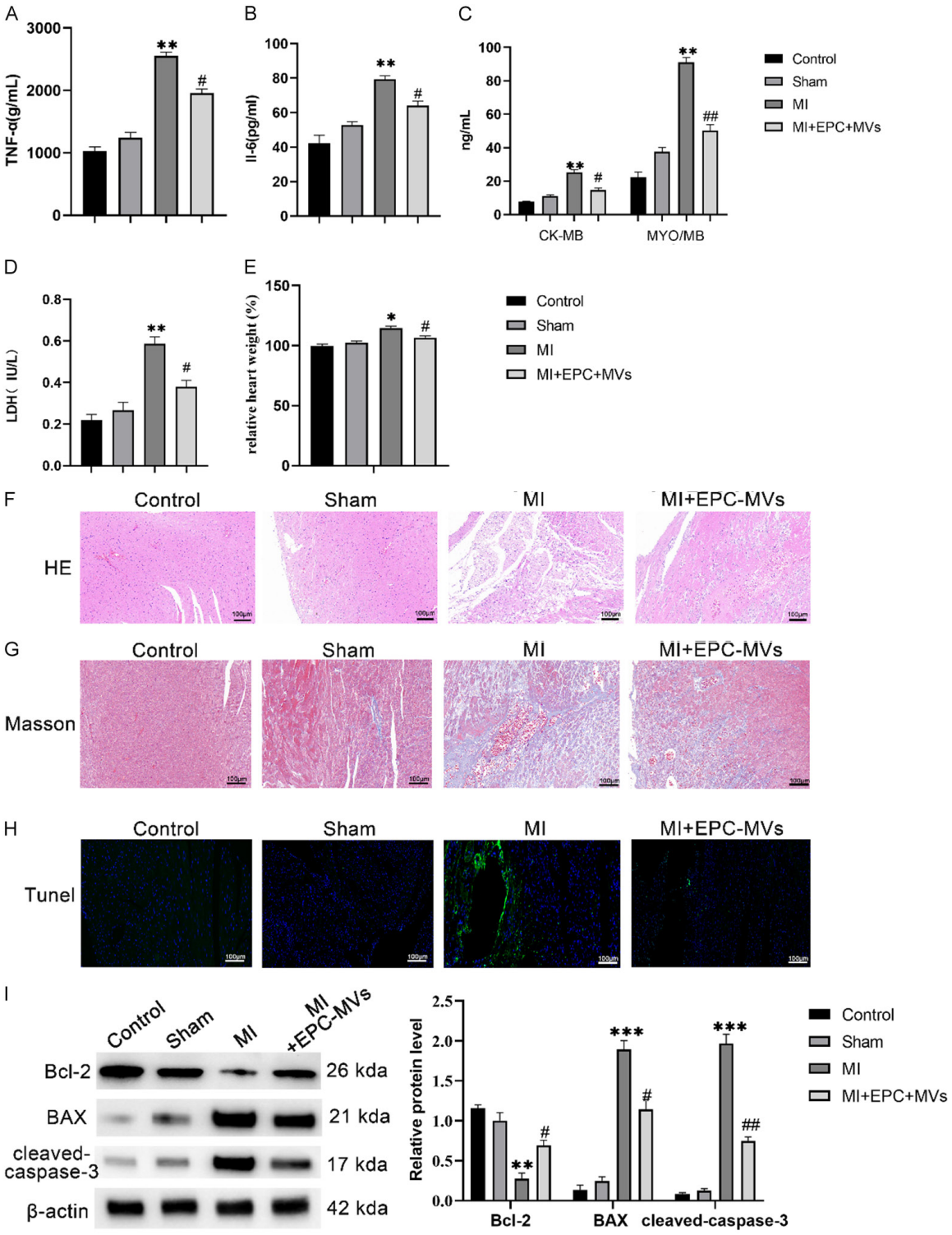


**Figure 2.** Effects of EPC-derived microvesicles (EPC-MVs) on MI injury. A. TNF-α levels measured by ELISA. B. IL-6 levels measured by ELISA. C. Creatine kinase-MB (CK-MB) and myoglobin/creatine kinase-MB (MYO/MB) levels measured byELISA. D. Lactate dehydrogenase (LDH) activity measured by ELISA. E. Relative heart weight ratio. F. H&E-stained cardiac tissue showing myocardial architecture (×15). Scale bar 100 μm. G. Masson's trichrome staining highlighting collagen deposition (×15). Scale bar 100 μm. H. TUNEL staining showing apoptotic cardiomyocytes (green) (×15). Scale bar 100 μm. I. Western blotting of Bcl-2, BAX, and cleaved caspase-3 expression, β-actin served as a loading control. n = 3. Data are presented as mean ± SEM. Statistical analysis: one-way ANOVA with Tukey's post hoc test. *P < 0.05, **P < 0.01, ***P < 0.001 vs. Sham; #P < 0.05, ##P < 0.01 vs. myocardial infarction (MI).

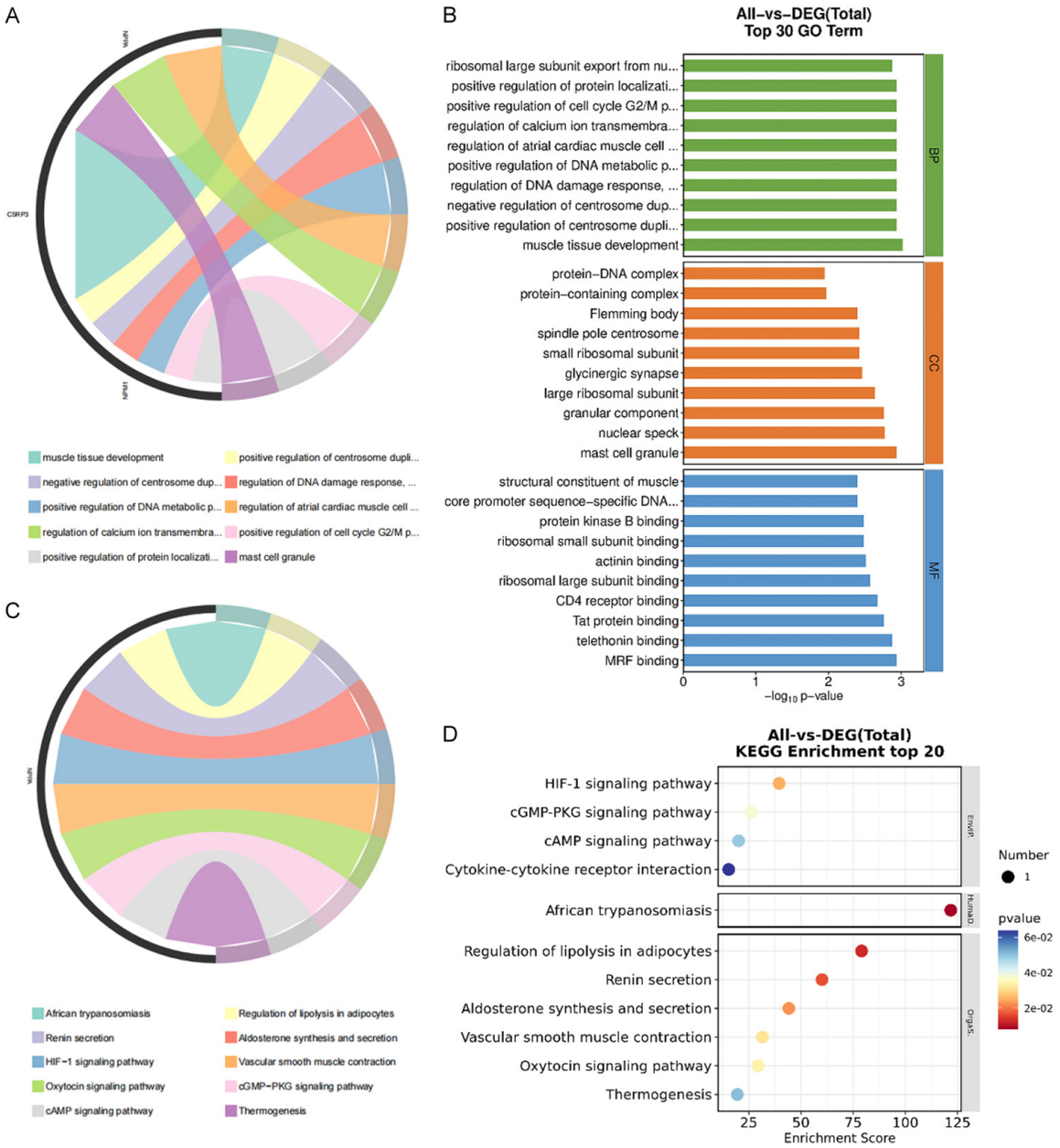


**Figure 3.** GO and KEGG metabolomic enrichment analysis showed biological process in left ventricular proteome after myocardial infarction. A. Chord diagram of enriched GO biological processes for Differentially expressed genes (DEGs). B. Top 30 enriched GO terms across biological process, cellular component, and molecular function, ranked by -$\log_{10}$ (*p*-value). C. Chord diagram showing representative DEGs associated with key KEGG pathways, including "HIF-1 signaling" and "Renin secretion". D. Top 20 enriched KEGG pathways ranked by enrichment score. Statistical analysis: two-tailed hypergeometric test with Benjamini-Hochberg correction for multiple testing.

being directly involved in the reparative pathways activated by EPC-MVs.

## Discussion

This study provided compelling evidence for the therapeutic potential of EPC-MVs in mitigating the adverse outcomes of MI. Our findings collectively demonstrated that EPC-MVs effectively counteract inflammation, apoptosis, and adverse tissue remodeling by modulating key regulatory proteins. The strength of these conclusions is supported by our rigorous methodology, particularly the exclusive use of bone mar-

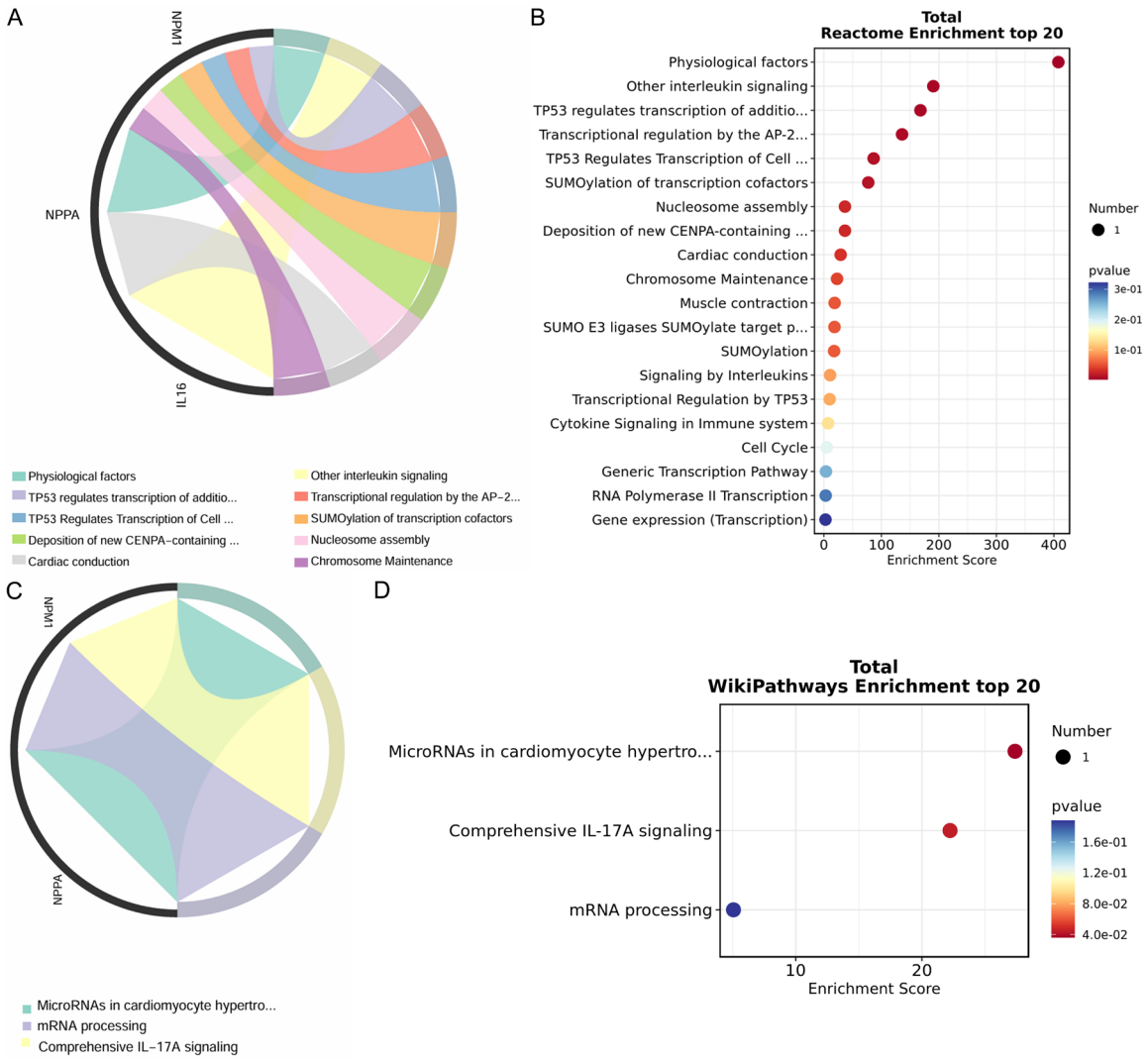


**Figure 4.** Through Reactome and Wikipathways enrichment analysis, the physiological process network and key pathways under the influence of metabolic changes were reflected. A. Chord diagram showing representative Reactome pathways enriched among Differentially expressed genes (DEGs). B. Top 20 enriched Reactome pathways ranked by enrichment score. C. Chord diagram showing WikiPathways enrichment results, highlighting pathways including “MicroRNAs in cardiomyocyte hypertrophy”, “Comprehensive IL-17A signaling”, and “mRNA processing”. D. Top 20 enriched WikiPathways displayed by enrichment score, with dot size and color representing DEG count and adjusted *p*-value, respectively. Statistical analysis: pathway enrichment using Reactome/WikiPathways tools with adjusted *p*-values by FDR correction.

row-derived EPCs ($CD34^+/VEGFR\text{-}2^+/CD133^+$), which ensures a pure, potent, and traceable source of therapeutic vesicles, consistent with our previous work [19, 20].

A key mechanism underlying this cardioprotective effect is the potent anti-inflammatory action of EPC-MVs. The MI model exhibited a characteristic inflammatory cascade, including elevated cytokines TNF-α and IL-6, and robust activation of the NLRP3 inflammasome pathway (NLRP3, Caspase-1, ASC). Given that inflammasome activation is a major contributor to secondary myocardial damage [21, 22], the marked suppression of these pathways by EPC-MVs highlights their critical therapeutic role. This was further validated by the significant reduction in IL-6, a pivotal mediator of post-infarction injury, confirming the broad anti-inflammatory capacity of EPC-MVs [23, 24].

In addition to their anti-inflammatory effects, EPC-MVs modulate proteins involved in myocardial stress and structural integrity. NPM1, a

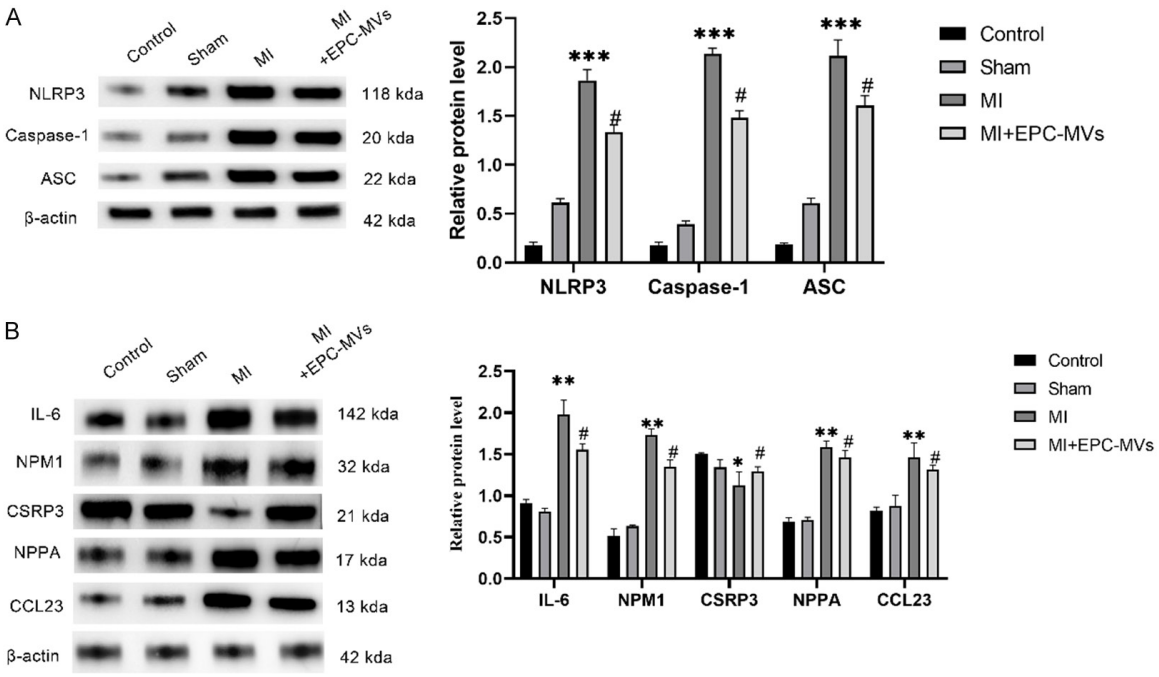


**Figure 5.** Effect of EPC-MVs on inflammatory and myocardial injury-related proteins in MI. A. Western blot analysis of NLRP3, Caspase-1, and ASC protein expression in myocardial tissues from control, sham, myocardial infarction (MI), and MI + endothelial progenitor cell-derived microvesicles (EPC-MVs) groups. β-actin served as a loading control. B. Western blot analysis of interleukin-6 (IL-6), nucleophosmin 1 (NPM1), cysteine and glycine-rich protein 3 (CSRP3), natriuretic peptide A (NPPA), and C-C motif chemokine ligand 23 (CCL23). β-actin served as a loading control. n = 3 biological replicates per group. Data presented as mean ± SEM. Statistical analysis: one-way ANOVA with Tukey's post hoc test. *P < 0.05, **P < 0.01, ***P < 0.001 vs. Sham; #P < 0.05 vs. myocardial infarction (MI).

stress-response protein upregulated during ischemic injury [25], was significantly reduced by EPC-MV treatment. This reduction was interpreted not as suppression of a protective factor, but rather as a resolution of the cellular stress that drives its upregulation. Furthermore, EPC-MVs restored levels of CSRP3, a protein crucial for cardiomyocyte architecture that was diminished post-MI [26], highlighting their direct role in preserving tissue integrity. In contrast, NPPA, while elevated post-MI, was unaffected by EPC-MVs, suggesting that these vesicles specifically target injury pathways rather than global hemodynamic stress responses.

Interestingly, EPC-MVs increased the chemokine CCL23, suggesting a functional shift from acute inflammation towards chronic tissue repair and beneficial immune modulation [24, 27].

Our comprehensive proteomic analysis offers a molecular framework that explains these functional outcomes. Pathway mapping by GO and KEGG analyses revealed that EPC-MVs modulate critical signaling networks, including the HIF-1, cGMP-PKG, and vascular smooth muscle contraction pathways. These pathways, known regulators of cellular stress responses and myocardial repair [28-30], provide a strong mechanistic basis for the favorable cardiac remodeling and functional recovery observed in our model.

This study has several limitations. First, all experiments were conducted in a murine model, which may not fully reflect human myocardial infarction. Second, proteomic analysis was confined to the left ventricle; given that myocardial infarction provokes a global cardiac response, this limitation may miss region-specific differences, and future studies should therefore encompass other cardiac regions to provide a comprehensive understanding of the systemic impact of EPC-MV therapy. Third, we did not compare EPC-MVs with other extracellular vesicle types such as exosomes, and a direct comparison with exosomes - the other major class of extracellular vesicles - is warranted to clarify the respective advantages of

different vesicle-based therapies in myocardial repair.

Future research should further investigate the long-term functional outcomes, biodistribution, and mechanisms of EPC-MV uptake. Additionally, standardization of EPC-MV production and evaluation under clinical-grade conditions are essential for future translation.

In conclusion, this study demonstrated that EPC-MVs confer robust cardioprotection in a preclinical MI model. The therapeutic effect is driven by a multifaceted mechanism, beginning with the modulation of critical signaling pathways, such as HIF-1 and cGMP-PKG. This, in turn, orchestrates the expression of key proteins - including CSRP3, NPM1, and NLRP3 inflammasome components - potently suppressing inflammation, attenuating apoptosis and fibrosis, and ultimately preserving myocardial integrity. By elucidating these mechanistic pathways, our findings position EPC-MVs as a highly promising cell-free therapeutic strategy and provide a solid rationale for their future clinical translation for patients with ischemic heart disease.

## Acknowledgements

This study was supported by the Natural Science Foundation of Hainan Province in 2023 (Grant No. 823RC577, Project Title: Proteomic Study on the Protective Mechanism of Endothelial Progenitor Cell Microvesicles against Myocardial Ischemia-Reperfusion Injury).

## Disclosure of conflict of interest

None.

**Address correspondence to:** Shenhong Gu, Department of General Practice, The First Affiliated Hospital of Hainan Medical University, 31 Longhua Road, Longhua District, Haikou 570100, Hainan, China. E-mail: renee388@163.com

## References

[1] Song Y, Bai Z, Zhang Y, Chen J, Chen M, Zhang Y, Zhang X, Mai H, Wang B, Lin Y and Gu S. Protective effects of endothelial progenitor cell microvesicles on Ang II–induced rat kidney cell injury. Mol Med Rep 2022; 25: 4.

[2] Fishbein GA, Fishbein MC, Wang J and Buja LM. Myocardial ischemia and its complications. Cardiovascular pathology. Elsevier; 2022. pp. 407-445.

[3] Kologrivova I, Shtatolkina M, Suslova T and Ryabov V. Cells of the immune system in cardiac remodeling: main players in resolution of inflammation and repair after myocardial infarction. Front Immunol 2021; 12: 664457.

[4] Ushakov A, Ivanchenko V and Gagarina A. Regulation of myocardial extracellular matrix dynamic changes in myocardial infarction and postinfarct remodeling. Curr Cardiol Rev 2020; 16: 11-24.

[5] Gold MR, Rickard J, Daubert JC, Cerkvenik J and Linde C. Association of left ventricular remodeling with cardiac resynchronization therapy outcomes. Heart Rhythm 2023; 20: 173-180.

[6] Xu J, Bai S, Cao Y, Liu L, Fang Y, Du J, Luo L, Chen M, Shen B and Zhang Q. miRNA-221-3p in endothelial progenitor cell-derived exosomes accelerates skin wound healing in diabetic mice. Diabetes Metab Syndr Obes 2020; 13: 1259-1270.

[7] Naserian S, Abdelgawad ME, Afshar Bakshloo M, Ha G, Arouche N, Cohen JL, Salomon BL and Uzan G. The TNF/TNFR2 signaling pathway is a key regulatory factor in endothelial progenitor cell immunosuppressive effect. Cell Commun Signal 2020; 18: 94.

[8] Schuh A, Liehn EA, Sasse A, Hristov M, Sobota R, Kelm M, Merx MW and Weber C. Transplantation of endothelial progenitor cells improves neovascularization and left ventricular function after myocardial infarction in a rat model. Basic Res Cardiol 2008; 103: 69-77.

[9] Huang H and Huang W. Regulation of endothelial progenitor cell functions in ischemic heart disease: new therapeutic targets for cardiac remodeling and repair. Front Cardiovasc Med 2022; 9: 896782.

[10] Guo Y, Tan J, Miao Y, Sun Z and Zhang Q. Effects of microvesicles on cell apoptosis under hypoxia. Oxid Med Cell Longev 2019; 2019: 5972152.

[11] Sun R, Wang X, Nie Y, Hu A, Liu H, Zhang K, Zhang L, Wu Q, Li K, Liu C, Zhang H, Zheng B, Li H, Xu H, Xu R, Fu H, Dai L, Jin R and Guo Y. Targeted trapping of endogenous endothelial progenitor cells for myocardial ischemic injury repair through neutrophil-mediated SPIO nanoparticle-conjugated CD34 antibody delivery and imaging. Acta Biomater 2022; 146: 421-433.

[12] Sheu JJ, Yeh JN, Sung PH, Chiang JY, Chen YL, Wang YT, Yip HK and Guo J. ITRI biofilm prevented thoracic adhesion in pigs that received myocardial ischemic induction treat-

ed by myocardial implantation of EPCs and ECSW treatment. Cell Transplant 2024; 33: 9636897241253144.
[13] Han Y, Yan J, Li ZY, Fan YJ, Jiang ZL, Shyy JY and Chien S. Cyclic stretch promotes vascular homing of endothelial progenitor cells via Acsl1 regulation of mitochondrial fatty acid oxidation. Proc Natl Acad Sci U S A 2023; 120: e2219630120.
[14] Gan F, Liu L, Zhou Q, Huang W, Huang X and Zhao X. Effects of adipose-derived stromal cells and endothelial progenitor cells on adipose transplant survival and angiogenesis. PLoS One 2022; 17: e0261498.
[15] Xu X, Zhang H, Li J, Chen Y, Zhong W, Chen Y and Ma X. Combination of EPC-EXs and NPC-EXs with miR-126 and miR-210 overexpression produces better therapeutic effects on ischemic stroke by protecting neurons through the Nox2/ROS and BDNF/TrkB pathways. Exp Neurol 2023; 359: 114235.
[16] Feng Z, Zhou J, Liu Y, Xia R, Li Q, Yan L, Chen Q, Chen X, Jiang Y, Chao G, Wang M, Zhou G, Zhang Y, Wang Y and Xia H. Epithelium- and endothelium-derived exosomes regulate the alveolar macrophages by targeting RGS1 mediated calcium signaling-dependent immune response. Cell Death Differ 2021; 28: 2238-2256.
[17] Tang YC, Hsiao JR, Jiang SS, Chang JY, Chu PY, Liu KJ, Fang HL, Lin LM, Chen HH, Huang YW, Chen YT, Tsai FY, Lin SF, Chuang YJ and Kuo CC. c-MYC-directed NRF2 drives malignant progression of head and neck cancer via glucose-6-phosphate dehydrogenase and transketolase activation. Theranostics 2021; 11: 5232-5247.
[18] Liao F, Liao Z, Zhang T, Jiang W, Zhu P, Zhao Z, Shi H, Zhao D, Zhou N and Huang X. ECFC-derived exosomal THBS1 mediates angiogenesis and osteogenesis in distraction osteogenesis via the PI3K/AKT/ERK pathway. J Orthop Translat 2022; 37: 12-22.
[19] Gu S, Zhang W, Chen J, Ma R, Xiao X, Ma X, Yao Z and Chen Y. EPC-derived microvesicles protect cardiomyocytes from Ang II-induced hypertrophy and apoptosis. PLoS One 2014; 9: e85396.
[20] Mai H, Huang Z, Zhang X, Zhang Y, Chen J, Chen M, Zhang Y, Song Y, Wang B, Lin Y and Gu S. Protective effects of endothelial progenitor cell microvesicles carrying miR-98-5p on angiotensin II-induced rat kidney cell injury. Exp Ther Med 2022; 24: 702.
[21] Xu M, Ye Z, Zhao X, Guo H, Gong X and Huang R. Deficiency of tenascin-C attenuated cardiac injury by inactivating TLR4/NLRP3/caspase-1 pathway after myocardial infarction. Cell Signal 2021; 86: 110084.
[22] Wang K, Zhou Y, Wen C, Du L, Li L, Cui Y, Luo H, Liu Y, Zeng L, Li S, Xiong L and Yue R. Protective effects of tetramethylpyrazine on myocardial ischemia/reperfusion injury involve NLRP3 inflammasome suppression by autophagy activation. Biochem Pharmacol 2024; 229: 116541.
[23] Mehta NN, deGoma E and Shapiro MD. IL-6 and cardiovascular risk: a narrative review. Curr Atheroscler Rep 2024; 27: 12.
[24] Zhang S, Zhang Y, Duan X, Wang B and Zhan Z. Targeting NPM1 epigenetically promotes postinfarction cardiac repair by reprogramming reparative macrophage metabolism. Circulation 2024; 149: 1982-2001.
[25] Oudot C, Gomes A, Nicolas V, Le Gall M, Chaffey P, Broussard C, Calamita G, Mastrodonato M, Gena P, Perfettini JL, Hamelin J, Lemoine A, Fischmeister R, Vieira HLA, Santos CN and Brenner C. CSRP3 mediates polyphenols-induced cardioprotection in hypertension. J Nutr Biochem 2019; 66: 29-42.
[26] Fu W, Ren H, Shou J, Liao Q, Li L, Shi Y, Jose PA, Zeng C and Wang WE. Loss of NPPA-AS1 promotes heart regeneration by stabilizing SFPQ-NONO heteromer-induced DNA repair. Basic Res Cardiol 2022; 117: 10.
[27] Karan D. CCL23 in balancing the act of endoplasmic reticulum stress and antitumor immunity in hepatocellular carcinoma. Front Oncol 2021; 11: 727583.
[28] Janbandhu V, Tallapragada V, Patrick R, Li Y, Abeygunawardena D, Humphreys DT, Martin EMMA, Ward AO, Contreras O, Farbehi N, Yao E, Du J, Dunwoodie SL, Bursac N and Harvey RP. Hif-1a suppresses ROS-induced proliferation of cardiac fibroblasts following myocardial infarction. Cell Stem Cell 2022; 29: 281-297, e212.
[29] Gao J, Feng W, Lv W, Liu W and Fu C. HIF-1/AKT signaling-activated PFKFB2 alleviates cardiac dysfunction and cardiomyocyte apoptosis in response to hypoxia. Int Heart J 2021; 62: 350-358.
[30] Hu M, Zhang X, Hu C, Ma ZG, Wang SS, Teng T, Zeng XF and Tang QZ. Isthmin-1 alleviates cardiac ischaemia/reperfusion injury through cGMP-PKG signalling pathway. Cardiovasc Res 2024; 120: 1051-1064.